

Skull Modulated Strategy to Intensify Tumor Treating Fields on Brain Tumor: a Finite Element Study

Yang Xin

Tsinghua University School of Aerospace Engineering

Penghao Liu (✉ liuph14@hotmail.com)

Peking Union Medical College Hospital <https://orcid.org/0000-0002-9100-1580>

Hao Xing

Peking Union Medical College Hospital

Xiaoyan Wen

Tsinghua University School of Aerospace Engineering

Yu Wang

Peking Union Medical College Hospital

Chunhua Hu

Tsinghua University School of Aerospace Engineering

Luming Li

Tsinghua University School of Aerospace Engineering

Wenbin Ma

Peking Union Medical College Hospital

Research Article

Keywords: Tumor treating fields, skull remodeling, cranioplasty, skull replacement, brain tumor, finite element analysis

Posted Date: April 28th, 2021

DOI: <https://doi.org/10.21203/rs.3.rs-470112/v1>

License: © ⓘ This work is licensed under a Creative Commons Attribution 4.0 International License.

[Read Full License](#)

Abstract

Purpose Tumor treating fields (TTFields) are a breakthrough in treating glioblastoma (GBM). Whereas, the intensity cannot be further enhanced, due to the limitation of scalp lesions. Skull remodeling (SR) surgery can elevate the treatment dose of TTFields in the intracranial foci. This study was aimed at exploring the characteristics of SR surgery towards TTFields augmentation. **Methods** The simplified multiple-tissue-layer model (MTL) model and realistic head (RH) model were reconstructed through finite element methods (FEM), to simulate the remodeling of the skull, which included skull drilling, thinning, and cranioplasty with PEEK, titanium, cerebrospinal fluid (CSF), connective tissue and autologous bone. **Results** Skull thinning could enhance the intensity of TTFields in the brain tumor, with a 10% of increase of average peritumoral intensity (API) by every 1 cm decrease in skull thickness. Cranioplasty with titanium accompanied the most enhancement of TTFields in the MTL model, but CSF was superior in TTFields enhancement when simulated in the RH model. Besides, API increased nonlinearly with the expansion of drilled burr holes. In comparison with the single drill replaced by titanium, 9 burr holes could reach 96.98% of enhancement in API, but it could only reach 63.08% of enhancement under craniectomy of 9-times skull defect area. **Conclusion** Skull thinning and drilling could enhance API, which was correlated with the number and area of skull drilling. Cranioplasty with highly conductive material could also augment API, but might not provide clinical benefits as expected. **Keywords** Tumor treating fields, skull remodeling, cranioplasty, skull replacement, brain tumor, finite element analysis

Introduction

Glioblastoma (GBM) is the most prevalent and malignant type of primary brain tumor, and patients suffer from poor life quality and limited survival. Despite the extension of median overall survival (mOS) up to 16 months by STUPP protocol¹. But the high recurrence rate usually leads to more restricted treatments and a worse prognosis². Although many pieces of research have presented promising efficacy in their preliminary phases, the majority of phase III clinical trials have failed, including cytotoxic drugs^{3,4}, targeted therapies⁵⁻⁷, immunotherapies^{8,9}, and oncolytic viruses¹⁰.

Tumor treating fields (TTFields) apply external alternating electric fields of intermediate frequency and relatively low intensity to inhibit cytogenesis. The current researchers believe that TTFields can impair mitotic spindle microtubule formation and intervene mitosis through the dielectrophoretic effect. Some also proposed the influence on the potential of the cell membrane, as well as cell migration and invasion¹¹. TTFields can also exert anti-tumor effects through biological pathways as apoptosis, autophagy, DNA damage repair, molecule transportation, and angiogenesis¹². To be noted, TTFields function extensively on solid tumors like ovarian cancer, breast cancer, lung cancer, mesothelioma, or even in the more malignant form like pancreatic cancer and GBM¹³⁻¹⁸. EF-11 is the first phase III trial for TTFields on recurrent GBM patients, which presented comparable results between TTFields and standard care¹⁹. The following real-world study, PRiDe and EF-19^{20,21}, testified their safety. In EF-14, TTFields combined with temozolomide (TMZ) further extended the mOS to 20.9 months in newly diagnosed GBM

patients²², which directly led to the approval by the U.S. Food and Drug Administration (FDA) and enrollment in the guidance, becoming the “fourth modality” in GBM treatment²³.

However, the clinical practice of TTFields is hindered by their thermal effects. The arrays of TTFields are required to closely adhere to the scalp of the patients to reach the maximal dosage of field intensity intracranially. Prior studies have proved that the anti-tumor toxicity was positively correlated with the applied field intensity²⁴. Also as shown in the clinical trials, the higher compliance and local field density accompanied better clinical benefits^{25, 26}. Yet, skin lesions on the scalp are commonly observed in the TTFields users, and could cause reduction in the applicable dosage of TTFields and patients’ compliance^{19, 22, 26}. Currently, this is the most prominent impediment for TTFields practices.

Though researchers have reported the heat transfer pattern^{27, 28}, to our knowledge, there has been no effective means of reducing heat production. Another solution of optimizing TTFields is to manipulate the conductivity and permittivity of the intermediate medium to elevate the intracranial dosage without altering the external electric voltage. Korshoej AR et al conducted in vitro simulation studies to prove that the skull remodeling (SR) by drilling, thinning, and craniectomy could intensify the local dosage. And they recently published the results of their phase I trial entitled OptimalTTF-1, in which SR surgery combined with TTFields and the physicians’ choice of cancer treatment could elongate the survival of recurrent GBM patients, compared to historical cohorts²⁹. Nevertheless, more detailed research on the modulations of SR surgery is required. Therefore, this research was aimed at exploring the relationships between the configurations of SR surgery and TTFields enhancement. Also, the implant of other bio-compatible materials during cranioplasty was simulated, and its effects on TTFields penetration were analyzed.

Methods

Mathematical model

The electric field distribution is approximated by applying the volume conductor model to numerically solve the derivative of Maxwell's electrodynamic equation under appropriate boundary conditions. TTFields were assumed quasi-stationary for the dielectric properties of biological tissues and the frequency of TTFields (200kHz) satisfied $\omega\epsilon \ll \sigma$, where σ was the real-valued conductivity, ϵ was the dielectric constant of tissue and ω was the angular frequency of TTFields. This implied that when calculating the strength and distribution of TTFields, the scalar electric potential φ could be approximated using Laplace's equation $\nabla(\sigma\nabla\varphi) = 0$.

In COMSOL, the major equations were as follows:

$$\begin{aligned}\nabla \cdot J &= Q, \\ J &= \sigma E + J_e, \\ E &= -\nabla V,\end{aligned}$$

Where J was the current density, Q was the charge, σ was the conductivity, E was the field strength, and J_e was the external current density.

Head model (simulated object)

To clarify the general distribution of intracranial electric fields under different skull thicknesses and implants, we generated a simplified multiple-tissue-layer (MTL) model in the shape of cuboid by COMSOL Multiphysics (see Figure 1). The MTL model reconstructed the multiple sectioned layers of the brain covered by TTFields, which were marked as the scalp, skull, cerebrospinal fluid (CSF), grey matter (GM), and white matter (WM), regardless of the complex configurations of gyri and sulci³⁰. The tumor in this model was set parallel to the center of the arrays of TTFields according to prior studies³¹⁻³³. The diameter of the tumor was 20 mm, the thickness of edema and invasion was 3mm, and the core represented necrosis.

The realistic head (RH) model was built from the head MRI data on the SimNIBS website (www.simnibs.org)³⁴, which was scanned from a young healthy male subject through 3.0T Philips Achieva equipped with a 32-channel head coil, including the high-resolution T1, T2 weighted images and diffusion Magnetic Resonance Imaging (MRI). Written consent was acquired on the open access and publication of his imaging data. We utilized the SimNIBS 3.0 to integrate the transformed imaging data. The headreco command was run to establish the three-dimensional head model. Then MIMICS Research, 3-Matic Research, and Materialise Magics were applied for model smoothing and mesh optimization (see Figure 2).

The brain tissue is of high complexity and the lower part of the head contributes minor influence to studying the supratentorial brain tumor. Therefore, the RH model needed to be further simplified accordingly. Meanwhile, each layer was smoothed, avoiding the nonspecific influence and time-

consuming brought by the complex configuration of WM and GM. The tumor was designed in the same way as that in the MTL model.

The settings of the numerical simulation

Although the TTFIELDS devices consist of two pairs of electrodes in an orthogonal position, we applied only one pair as 3x3 arrays to exclude the influences of anisotropy and focused mainly on the enhancement on the intensity of electric field. A total of 18 sites (C1-C6, FC1-FC6, CP1-CP6) were selected, which were all preset in SimNIBS (see Figure 1). The arrays were designed as cylinders with the diameter of 2cm, the thickness of 1mm, and the gel of 1mm thick. The current frequency was 200 kHz and the intensity was 100 mA in sin signal. Since the more aggressive cancer cells usually aggregate in the peritumoral region, we calculated the average field intensity per volume in the peritumoral region, entitled "average peritumoral intensity (API)" as a representation of intracranial dosage of TTFIELDS.

The thickness of the skull was adjusted in the simplified MTL model and the corresponding field intensity was calculated to simulate the effects of skull thinning on TTFIELDS enhancement. Moreover, in the RH model, the commonly used bio-compatible materials including titanium and polyetheretherketone (PEEK) were simulated as implants during cranioplasty. CSF, connective tissue, and autologous bone were also taken as control. The conductivity of titanium is 2.34×10^6 S/m with a relative dielectric constant of 10, the conductivity of PEEK is 1×10^{-15} S/m with a relative dielectric constant of 3.2, and the conductivity of cortical bone is $1.0\text{-}2.1 \times 10^{-2}$ S/m with a relative dielectric constant of 200³⁵. We also altered the arranged pattern and the size of skull drilling to explore the relationship between the configurations of SR surgery and the effective dosage of TTFIELDS in the peritumoral region.

The TTFIELDS were solved using the COMSOL Multiphysics software. Domain Solver was applied to calculate the field intensity. In addition, we conducted a sensitivity analysis to determine the variations in the conductivities of tissues, which affected the electric field in the tumor. The electric parameters were listed in Supplementary Table 1[34,35].

Validation of Finite Element Methods (FEM)

In order to verify the reliability of the FEM calculations, we conducted validation experiments using pork tissues (fatty and lean meat). A voltage signal was applied to the outside of the tissue, while the potentials at different sites in the tissue were measured using a differential probe, and the results were compared with those of the FEM calculations to plot the validation curves. In addition, for the materials, such as the bone, PEEK and titanium, which were involved in this study, a similar approach was applied to simulate the aforementioned cranioplasty surgery model in vitro. The potentials in the pork tissues were measured using a differential probe, compared with the FEM calculation results, and the validation curves were plotted.

Results

Model validation

To validate the reliability of finite element calculation in the MTL model, a simplified experimental device was established. We put different types of pork tissues into special containers and applied voltage signals as Supplementary Figure 1A, 1B. The electrical potential at different locations was measured with differential probe and calculated in COMSOL using the electric parameters listed in Supplementary Table 1, to compare the calculation and experiment as Supplementary Figure 1C and 1D. The difference between the experimental results and the calculated results was within an acceptable range.

We then simulated the cranioplasty model in vitro with pork tissue, using bone plates, PEEK and titanium plates to fill the gap between the pork tissue and the electrodes. The parameters of each material used in the experiment were listed in Supplementary Table 3. A fixed voltage of ± 20 V was applied to both electrodes, and a differential probe was used to measure the potentials at specific locations in the tissue, as shown in Supplementary Figure 2A-F), which were located at 20 mm, 10 mm, 0 mm, -10 mm, and -20 mm from the center of the tissue (the right was positive, Supplementary Figure 2F). The experimental data were compared with the FEM calculations, and the validation curves were drawn as shown in the Supplementary Figure 2G-L). The deviations were within the acceptable range.

The effects of tissue conductivity on the API

The primary hypothesis is that each layer with different conductivity might have the distinct influence on the field intensity. The simulation was performed in the established head model, with simplified 5 layers of tissue, including the scalp, skull, CSF, GM, and WM. $\Delta E/\Delta\sigma$ of each tissue was calculated to represent the direction and extent of influence on TTFields (Figure 3A). Among the investigated tissues, the skull showed the most prominent effects on TTFields, and the rest of those tissues might exert similar negligible effects on TTFields. Besides, only the conductivity of the skull presented a positive relationship with TTFields enhancement. In other words, the increase of skull conductivity could more efficiently enhance the intracranial treatment dosage of TTFields. We conducted sensitivity analysis by changing the conductivity of each tissue within specific ranges listed in Supplementary Table 1. The skull conductivity had the greatest effect on the API, followed by the tumor itself. However, other tissues exhibited subtle effects on the API. And in accordance with the prior findings, only the skull conductivity presented a positive effect on the API.

Skull thinning augmented the API

When simulating skull thinning in the MTL model, we considered two conditions: group 1. the total size of the head remained the same, while the defect area was replaced by connective tissue, as seen in most patients who underwent a secondary resection for the recurrent brain lesions; group 2. the other tissues were not altered along with the skull thinning, and the total size of the head was reduced accordingly. The thickness of the skull was set as a decreasing sequence from 6mm to 0mm, and API was calculated separately for group 1 and group 2 (see Table 1). The results demonstrated that the extent of skull thinning correlated positively with the increase in API, with an average 10% enhancement in the field

intensity as every 1mm reduction of skull thickness. The difference between group 1 and group 2 remained minor (below 2%) before the complete removal of the skull, which meant that the total size of the head could be neglected during TTFields simulation on skull thinning.

Table 1. The effects of skull thinning on peritumoral field intensity

Skull thickness (mm)	Field enhancement in Group 1 (E/V·m ⁻¹)	Field enhancement in Group 2 (E/V·m ⁻¹)	Difference between group 1 and 2 (%)
6	258.23	258.23	0.00
5	281.67	278.70	1.05
4	308.10	302.72	1.75
3	339.05	332.53	1.92
2	376.18	370.78	1.44
1	422.84	423.99	0.27
0	487.83	518.13	6.21

Cranioplasty with bio-compatible material and the configurations of the burr holes affected the API

First, we simulated a single burr hole in the MTL model, which was the same size as the electrode, and placed at the center of the 3 3 array. The electric parameters of PEEK and titanium were incorporated as the repairing material. Also based on our observation in patients under repeated brain surgeries, the defects of the skull would be filled by tissue fluids shortly after surgeries, while could also be replaced by connective tissue. Thus, the data of CSF and connective tissue were also integrated as a simulation for the patients without skull repairing, and autologous bone was considered as the baseline. According to the FEM results, titanium contributed most to the enhancement of TTFields, followed by CSF, the connective tissue, autologous bone and PEEK (see Figure 4).

Furthermore, we explored whether the size of the burr holes could enhance API under the condition of cranioplasty surgery. When linearly increased the size of the burr holes replaced by different materials, we noticed that the more area implanted with high-conductivity materials, such as titanium, CSF, and connective tissue, the higher API could be reached. By contrast, API grew negatively with the increase of the implantation of PEEK. Besides, we created 9 burr holes corresponding to the size and locations of electrodes on the skull and calculated the alteration in API. The results presented a maximum enhancement of 96.98% with the implanted titanium, followed by CSF, connective tissue, and PEEK (see Supplementary Table 2).

Then, a similar simulation of the skull remodeling was conducted in the RH model, under a single burr hole and nine burr holes separately. In both patterns, however, the connective tissue offered the strongest enhancement to API, followed by the CSF, titanium, and PEEK (see Figure 5), which was contradicted the results in the MTL model. Moreover, compared to a single burr, nine burr holes in an array provided better augmentation in API, which was in accordance with that of the MTL model.

The skull drilling of a single hole compared to nine holes, and cranioplasty with different planted material were simulated in the RH model. In both drilling patterns, the connective tissue ranked the highest in

TTFields enhancement, followed by CSF, the titanium, autologous bone, and PEEK. And nine burr holes in an array offered more enhancement to API, compared to a single burr hole in all models.

Discussion

This study investigated the effects of skull modulation on the enhancement of intracranial TTFields intensity, including adjusting different configurations of SR surgery or performing cranioplasty surgery with replaced materials. Skull thinning, drilling, and skull replacement with high-conductivity materials could all increase API.

The distribution of TTFields was predominantly determined by the local conductivities of brain tissues, which was also the prerequisite hypothesis of this research³⁶. The dense skull offered the toughest impediment to the penetration of the external electric fields. Interestingly, other brain tissues except for the skull presented negative relationships with TTFields. This phenomenon might be due to “the charge shielding effects” that induced converse electric fields against the external TTFields. Therefore, the elevation of conductivity within these tissues could cause a decrease in the intracranial dosage of electric fields. As Lang S et al reported that peritumoral edema could hinder the TTFields penetration, and 6mm of edema blocked 52% of intracranial electric field intensity³⁷. Hence manipulating the conductivity of the brain and skull could be a potential facilitation to TTFields, for instance, alleviating the brain edema through Bevacizumab and steroids, or alternating the configurations and materials of the skull.

In comparison between the two commonly implanted materials, titanium and PEEK, the former offered more intracranial augmentation to TTFields, and the intensity was elevated as the increase of the replaced area, but the growth rate of API declined as the skull defects further expanded. And we considered that the excessive implantation not only accompanied higher risks of infection, and might not provide clinical benefits as expected. Parameters of the CSF and connective tissue were also incorporated as reference models, because the resected lesions would soon be filled with fluid, and a stepwise re-organization by connective tissues. The conductivity of titanium is far larger than that of CSF, and the titanium implant offered much stronger augmentation to TTFields in the MTL model. However, their differences in the intensity of intracranial electric fields were only about 3% in the RH model. The distinction might lie in the complex configurations of gyri and sulci, which could generate more shielding charges against the external electric fields. Therefore, theoretically, titanium might not be as effective as what was observed in the RH model, but it requires further evidences in real patients.

Korshoej AR reported in 2016 that SR surgery could enhance electric fields in the tumor regions³⁸. Based on the MRI data of two patients with superficial or deep brain tumors, they stated that craniectomy could elevate the dosage of TTFields in both models, especially for the superficial tumor, and the size and shape of the burr holes affected the peritumoral electric intensity³⁸. The primary results further supported their following clinical trials³⁹. In the phase I clinical trial OptimalTTF-1, 15 GBM patients with the first recurrence were enrolled. They all received a second brain tumor debulk surgery and other physician’s choices of therapy³⁹. The tumors were all near the surface of the brain and 4 patients did not receive

TTFIELDS due to personal reasons. Three drilling patterns were applied with significantly prolonged median progression free survival (mPFS) and mOS (mPFS, 4.6 months; 6-month PFS rate, 36%; mOS, 15.5 months)²⁹. To clarify the exact augmentation of SR surgery to TTFIELDS, one phase II clinical trial (NCT04223999) is ongoing.

Admittedly, the authenticity was compromised by the simplified MTL model and RH model. In particular, the RH model was constructed based on the imaging data of a healthy subject, and we simplified the model to eliminate as many individualized features as possible, then a virtual tumor was manually placed to shape a relatively standardized realistic head model^{40,41}. This was mainly for avoiding the confounding factors that affected TTFIELDS dosimetry other than electric field strength, such as head shape and tumor morphology⁴². Nevertheless, due to the complex anatomy of the head, variations in neuro-fiber topology, and the isotropic conductivity distribution, orthogonal electric fields with 2 pairs of transducer arrays might introduce considerable correlations which were indexed as fractional anisotropy (FA)^{40,42}. Even at the optimal electrode position with maximum TTFIELDS intensity, FA could still bias the pattern of the electric fields³⁶. Thus, we applied only 1 pair of 3×3 transducer arrays in the left-right field direction parallel to the tumor. Diffusion tensor imaging (DTI) was not available for the subject, and detailed simulation concerning FA could not be acquired. Moreover, only one RH model might not be representative for all patients. These limitations all indicated an urgent need for prospective simulation studies on real patients.

Another limitation was the lack of thermal simulation on the head model. Despite broad clinical applications in cranioplasty, titanium is notorious for its skin burnt under heat or direct sunlight exposure. The alternating electric fields might also increase the heat produced by titanium. Also, the skull drilling is an invasive procedure, which warrants precise scheme and design, but we only simulated some of the occasions where the burr holes were set corresponding to the electrodes. Further exploration on the configurations of skull drilling and the safety of cranioplasty with other replaced materials are still required for further clinical applications.

Besides, considering the edge effect of the transducer array, our research did not involve the influence of the relative position of electrodes and the tumor on the peritumoral field intensity. In our simulation, we set the tumor fixed deeply and directly below the center of the electrode array, in which case we believed that the edge effect of electrodes had subtle impact on the peritumoral electrical fields⁴⁰.

Our research was aimed at the clinical optimization of TTFIELDS. Except for the method of altering skull conductivity as mentioned above, reducing the heat produced by electrodes are also essential (see Fig. 6), which is the key problem hindering its usage. Researches have focused on simulating the heat transfer pattern of TTFIELDS²⁸, but to our knowledge, none reported feasible solutions. Further studies might overcome this issue from the perspective of materials. Besides, although the new version of TTFIELDS has facilitated patients' life, many still complained about carrying the battery⁴³. From the perspective of thermal effects and life quality, implantable electrodes embedded in the skull or brain parenchyma, and the implantable batteries, which are similar to the design of cardiac pacemakers or deep brain stimulation

with batteries placed in the chest, could both increase the compliance of patients. As for the clinical practices, the current application of TTFields urgently requires appropriate criteria for evaluation. The clinical trials of TTFields mainly used scales like Mini-Mental Status Exam (MMSE), EORTC quality-of-life questionnaire core-30 (QLQ-C30), and BN20 to assess life quality and functions, and used Macdonald, or RANO criteria to assess the radiological progression of GBM patients treated with TTFields^{44, 45}. But there were reports of delayed response to TTFields as well⁴⁵. It is still required to verify in an extended population whether the established evaluation scales could represent the responses to TTFields, whether there is also pseudoprogression during the treatment, and whether there are other predictive factors, such as blood or imaging biomarkers and local minimum dose density (LMiDD)²⁵. Finally, as more studies attempting to reveal the anti-tumor mechanisms of TTFields, combinatory treatment regimens are also under consistent investigation⁴⁶. The upcoming studies could be focused on answering these questions.

The design of current TTFields that are applied in the clinic warrants further optimization, including better temperature control of the electrodes, performing SR surgery to enhance TTFields, and managing peritumoral edema to minimize its blocking effects. The devices also warrant further optimizing so that they can be lighter to carry, have implantable generators and electrodes, and be more durable in usage. Predictive factors from serum biomarkers and imaging markers are also required, and more combinatory regimens to augment TTFields should be further explored.

Conclusion

This research established the simplified MTL model and RH model through FEM analysis to simulate the process of SR surgery. This was the first research to propose the possibility of utilizing high-conductivity material like titanium in cranioplasty surgery to facilitate TTFields, but the results still needed to be further validated in terms of safety and applicability. Also, skull thinning and drilling could both enhance the electric field intensity in the peritumoral region. The larger number and area of burr holes could elevate the API. Future studies should be more focused on the clinical optimization of TTFields, including specifically altering the conductivity of skull and brain tissue, reducing thermal effects of electrodes, optimizing the clinical evaluation of patients treated with TTFields, and exploring more potentials in combinatory therapies.

Declarations

Funding

This work was funded by the [Tsinghua University Initiative Scientific Research Program] under Grant [number 20191080597]; [Tsinghua University-Peking Union Medical College Hospital Initiative Scientific Research Program] under Grant [number 2019ZLH101].

Conflict of interest

The authors declare that they have no conflict of interest.

Availability of data and material

Not applicable

Code availability

Not applicable

Ethics approval

Not applicable

Consent to participate

Written consent was acquired on the open access and publishment of his imaging data (www.simnibs.org).

Consent for publication

All authors agreed on the publication of this article.

Author's contributions

XY and PL designed the research; XY and XW conducted the simulation and calculation; XY and PL wrote and revised the article; CH supervised the study protocol and provide guidance in model validation; WM, YW, and HX provided clinical expertise in TTFIELDS application and SR surgery; LL and CH provide mechanical expertise in TTFIELDS design; LL provided funding and correspondence to this article. All authors have read and agreed to the published version of the manuscript.

Acknowledgment

We thank Yuge Yao from the Department of Energy and Power Engineering, Tsinghua University for revising the methods and language editing.

References

1. Stupp R, Mason WP, van den Bent MJ et al (2005) Radiotherapy plus concomitant and adjuvant temozolomide for glioblastoma. *N Engl J Med* 352:987–996. . DOI: 10.1056/NEJMoa043330
2. Weller M, Tabatabai G, Kästner B et al (2015) MGMT Promoter Methylation Is a Strong Prognostic Biomarker for Benefit from Dose-Intensified Temozolomide Rechallenge in Progressive Glioblastoma: The DIRECTOR Trial. *Clinical cancer research: an official journal of the American Association for Cancer Research* 21:2057–2064. DOI:10.1158/1078-0432.Ccr-14-2737. 2015/02/07.

3. Wick W, Gorlia T, Bendszus M et al. Lomustine and Bevacizumab in Progressive Glioblastoma. *The New England journal of medicine* 2017; 377: 1954–1963. 2017/11/16. DOI: 10.1056/NEJMoa1707358
4. Gilbert MR, Wang M, Aldape KD et al (2013) Dose-dense temozolomide for newly diagnosed glioblastoma: a randomized phase III clinical trial. *Journal of clinical oncology: official journal of the American Society of Clinical Oncology* 31:4085–4091. . DOI: 10.1200/jco.2013.49.6968
5. Westphal M, Heese O, Steinbach JP et al (2015) A randomised, open label phase III trial with nimotuzumab, an anti-epidermal growth factor receptor monoclonal antibody in the treatment of newly diagnosed adult glioblastoma. *European journal of cancer (Oxford England: 1990)* 51:522–532. . DOI: 10.1016/j.ejca.2014.12.019
6. Gilbert MR, Dignam JJ, Armstrong TS et al (2014) A randomized trial of bevacizumab for newly diagnosed glioblastoma. *N Engl J Med* 370:699–708. . DOI: 10.1056/NEJMoa1308573
7. Batchelor TT, Mulholland P, Neyns B et al (2013) Phase III randomized trial comparing the efficacy of cediranib as monotherapy, and in combination with lomustine, versus lomustine alone in patients with recurrent glioblastoma. *Journal of clinical oncology: official journal of the American Society of Clinical Oncology* 31:3212–3218. . DOI: 10.1200/jco.2012.47.2464
8. Liao LM, Ashkan K, Tran DD et al (2018) First results on survival from a large Phase 3 clinical trial of an autologous dendritic cell vaccine in newly diagnosed glioblastoma. *Journal of translational medicine* 16:142. . DOI: 10.1186/s12967-018-1507-6
9. Narita Y, Arakawa Y, Yamasaki F et al (2019) A randomized, double-blind, phase III trial of personalized peptide vaccination for recurrent glioblastoma. *Neurooncology* 21:348–359. . DOI: 10.1093/neuonc/noy200
10. Westphal M, Ylä-Herttuala S, Martin J et al. Adenovirus-mediated gene therapy with sitimagene ceradenovec followed by intravenous ganciclovir for patients with operable high-grade glioma (ASPECT): a randomised, open-label, phase 3 trial. *The Lancet Oncology* 2013; 14: 823–833. 2013/07/16. DOI: 10.1016/s1470-2045(13)70274-2
11. Carrieri FA, Smack C, Siddiqui I et al (2020) Tumor Treating Fields: At the Crossroads Between Physics and Biology for Cancer Treatment. *Frontiers in oncology* 10:575992. . DOI: 10.3389/fonc.2020.575992
12. Rominiyi O, Vanderlinden A, Clenton SJ et al. Tumour treating fields therapy for glioblastoma: current advances and future directions. *British journal of cancer* 2020 2020/11/05. DOI: 10.1038/s41416-020-01136-5
13. Voloshin T, Munster M, Blatt R et al (2016) Alternating electric fields (TTFields) in combination with paclitaxel are therapeutically effective against ovarian cancer cells in vitro and in vivo. *International journal of cancer* 139:2850–2858. . DOI: 10.1002/ijc.30406
14. Benson L (2018) Tumor Treating Fields Technology: Alternating Electric Field Therapy for the Treatment of Solid Tumors. *Semin Oncol Nurs* 34:137–150. DOI:10.1016/j.soncn.2018.03.005. 2018/04/11.

15. Giladi M, Schneiderman RS, Porat Y et al (2014) Mitotic disruption and reduced clonogenicity of pancreatic cancer cells in vitro and in vivo by tumor treating fields. *Pancreatology: official journal of the International Association of Pancreatology (IAP)* [et al] 14:54–63. . DOI: 10.1016/j.pan.2013.11.009
16. Karanam NK, Srinivasan K, Ding L et al. Tumor-treating fields elicit a conditional vulnerability to ionizing radiation via the downregulation of BRCA1 signaling and reduced DNA double-strand break repair capacity in non-small cell lung cancer cell lines. *Cell death & disease* 2017; 8: e2711. 2017/03/31. DOI: 10.1038/cddis.2017.136
17. Giladi M, Weinberg U, Schneiderman RS et al (2014) Alternating electric fields (tumor-treating fields therapy) can improve chemotherapy treatment efficacy in non-small cell lung cancer both in vitro and in vivo. *Seminars in oncology* 41(Suppl 6):S35–S41. . DOI: 10.1053/j.seminoncol.2014.09.006
18. Ceresoli GL, Aerts JG, Dziadziuszko R et al (2019) Tumour Treating Fields in combination with pemetrexed and cisplatin or carboplatin as first-line treatment for unresectable malignant pleural mesothelioma (STELLAR): a multicentre, single-arm phase 2 trial. *The Lancet Oncology* 20:1702–1709. . DOI: 10.1016/s1470-2045(19)30532-7
19. Stupp R, Wong ET, Kanner AA et al (2012) NovoTTF-100A versus physician's choice chemotherapy in recurrent glioblastoma: a randomised phase III trial of a novel treatment modality. *European journal of cancer (Oxford England: 1990)* 48:2192–2202. . DOI: 10.1016/j.ejca.2012.04.011
20. Mrugala MM, Engelhard HH, Dinh Tran D et al (2014) Clinical practice experience with NovoTTF-100A system for glioblastoma: The Patient Registry Dataset (PRiDe). *Seminars in oncology* 41(Suppl 6):S4–Ss13. . DOI: 10.1053/j.seminoncol.2014.09.010
21. Jay-Jiguang Zhu RTOD, Goldlust S, Ram Z (2020) CTNI-77-EF-19, a post-approval registry study of Tumor Treating Fields (TTFields) o recurrent glioblastoma (rGBM). *Neuro-Oncology* 22:ii60. DOI:<https://doi.org/10.1093/neuonc/noaa215.243>
22. Stupp R, Taillibert S, Kanner A et al (2017) Effect of Tumor-Treating Fields Plus Maintenance Temozolomide vs Maintenance Temozolomide Alone on Survival in Patients With Glioblastoma: A Randomized Clinical Trial. *Jama* 318:2306–2316. . DOI: 10.1001/jama.2017.18718
23. Mun EJ, Babiker HM, Weinberg U et al (2018) Tumor-Treating Fields: A Fourth Modality in Cancer Treatment. *Clinical cancer research: an official journal of the American Association for Cancer Research* 24:266–275. . DOI: 10.1158/1078-0432.Ccr-17-1117
24. Kirson ED, Gurvich Z, Schneiderman R et al (2004) Disruption of cancer cell replication by alternating electric fields. *Cancer research* 64:3288–3295. 2004/05/06
25. Ballo MT, Urman N, Lavy-Shahaf G et al (2019) Correlation of Tumor Treating Fields Dosimetry to Survival Outcomes in Newly Diagnosed Glioblastoma: A Large-Scale Numerical Simulation-Based Analysis of Data from the Phase 3 EF-14 Randomized Trial. *Int J Radiat Oncol Biol Phys* 104:1106–1113. . DOI: 10.1016/j.ijrobp.2019.04.008
26. Kesari S, Ram Z (2017) Tumor-treating fields plus chemotherapy versus chemotherapy alone for glioblastoma at first recurrence: a post hoc analysis of the EF-14 trial. *CNS oncology* 6:185–193. .

DOI: 10.2217/cns-2016-0049

27. Gentilal N, Miranda PC (2020) Heat transfer during TTFields treatment: Influence of the uncertainty of the electric and thermal parameters on the predicted temperature distribution. *Comput Methods Programs Biomed* 196:105706. . DOI: 10.1016/j.cmpb.2020.105706
28. Gentilal N, Salvador R, Miranda PC (2019) Temperature control in TTFields therapy of GBM: impact on the duty cycle and tissue temperature. *Physics in medicine biology* 64:225008. . DOI: 10.1088/1361-6560/ab5323
29. Korshoej AR, Lukacova S, Lassen-Ramshad Y et al (2020) OptimalTTF-1: Enhancing tumor treating fields therapy with skull remodeling surgery. A clinical phase I trial in adult recurrent glioblastoma. *Neurooncol Adv* 2:vdaa121. . DOI: 10.1093/noajnl/vdaa121
30. Sun YS. Direct-Current Electric Field Distribution in the Brain for Tumor Treating Field Applications: A Simulation Study. *Computational and mathematical methods in medicine* 2018; 2018: 3829768. . DOI: 10.1155/2018/3829768
31. Miranda PC, Mekonnen A, Salvador R et al (2014) Predicting the electric field distribution in the brain for the treatment of glioblastoma. *Phys Med Biol* 59:4137–4147. DOI:10.1088/0031-9155/59/15/4137. 2014/07/09.
32. Wenger C, Salvador R, Basser PJ et al. Modeling Tumor Treating fields (TTFields) application within a realistic human head model. *Annual International Conference of the IEEE Engineering in Medicine and Biology Society IEEE Engineering in Medicine and Biology Society Annual International Conference* 2015; 2015: 2555–2558. . DOI: 10.1109/embc.2015.7318913
33. Bomzon Z, Hershkovich HS, Urman N et al. Using computational phantoms to improve delivery of Tumor Treating Fields (TTFields) to patients. *Annual International Conference of the IEEE Engineering in Medicine and Biology Society IEEE Engineering in Medicine and Biology Society Annual International Conference* 2016; 2016: 6461–6464. . DOI: 10.1109/embc.2016.7592208
34. Thielscher A, Antunes A, Saturnino GB Field modeling for transcranial magnetic stimulation: a useful tool to understand the physiological effects of TMS?., *IEEE EMBS 2015, Milano, Italy* 2015
35. K X-j (2006) Discussion on Dielectric Constant of Metal. *Journal of Sichuan University of Science Engineering (Natural Science Edition)* 2:75–78
36. Korshoej AR, Hansen FL, Thielscher A et al. Impact of tumor position, conductivity distribution and tissue homogeneity on the distribution of tumor treating fields in a human brain: A computer modeling study. *PloS one* 2017; 12: e0179214. 2017/06/13. DOI: 10.1371/journal.pone.0179214
37. Lang ST, Gan LS, McLennan C et al (2020) Impact of Peritumoral Edema During Tumor Treatment Field Therapy: A Computational Modelling Study. *IEEE Trans Bio-med Eng* 67:3327–3338. . DOI: 10.1109/tbme.2020.2983653
38. Korshoej AR, Saturnino GB, Rasmussen LK et al (2016) Enhancing Predicted Efficacy of Tumor Treating Fields Therapy of Glioblastoma Using Targeted Surgical Craniectomy: A Computer Modeling Study. *PloS one* 11:e0164051. . DOI: 10.1371/journal.pone.0164051

39. Korshoej AR, Mikic N, Hansen FL et al. Enhancing Tumor Treating Fields Therapy with Skull-Remodeling Surgery. The Role of Finite Element Methods in Surgery Planning. *Conf Proc IEEE Eng Med Biol Soc* 2019; 2019: 6995–6997. DOI: 10.1109/EMBC.2019.8856556
40. Korshoej AR, Hansen FL, Mikic N et al (2018) Importance of electrode position for the distribution of tumor treating fields (TTFields) in a human brain. Identification of effective layouts through systematic analysis of array positions for multiple tumor locations. *PLoS One* 13:e0201957. . DOI: 10.1371/journal.pone.0201957
41. Wenger C, Miranda PC, Salvador R et al (2018) A Review on Tumor-Treating Fields (TTFields): Clinical Implications Inferred From Computational Modeling. *IEEE Rev Biomed Eng* 11:195–207. . DOI: 10.1109/rbme.2017.2765282
42. Korshoej AR, Sorensen JCH, von Oettingen G et al (2019) Optimization of tumor treating fields using singular value decomposition and minimization of field anisotropy. *Phys Med Biol* 64:04NT03. . DOI: 10.1088/1361-6560/aafe54
43. Onken J, Goerling U, Heinrich M et al (2019) Patient Reported Outcome (PRO) Among High-Grade Glioma Patients Receiving TTFields Treatment: A Two Center Observational Study. *Front Neurol* 10:1026. . DOI: 10.3389/fneur.2019.01026
44. Trusheim J, Dunbar E, Battiste J et al. A state-of-the-art review and guidelines for tumor treating fields treatment planning and patient follow-up in glioblastoma. *CNS oncology* 2017; 6: 29–43. 2016/09/16. DOI: 10.2217/cns-2016-0032
45. Vymazal J, Wong ET. Response patterns of recurrent glioblastomas treated with tumor-treating fields. *Seminars in oncology* 2014; 41 Suppl 6: S14-24. 2014/09/13. DOI: 10.1053/j.seminoncol.2014.09.009
46. Karanam NK, Story MD. An overview of potential novel mechanisms of action underlying Tumor Treating Fields-induced cancer cell death and their clinical implications. *International journal of radiation biology* 2020: 1–11. . DOI: 10.1080/09553002.2020.1837984

Figures

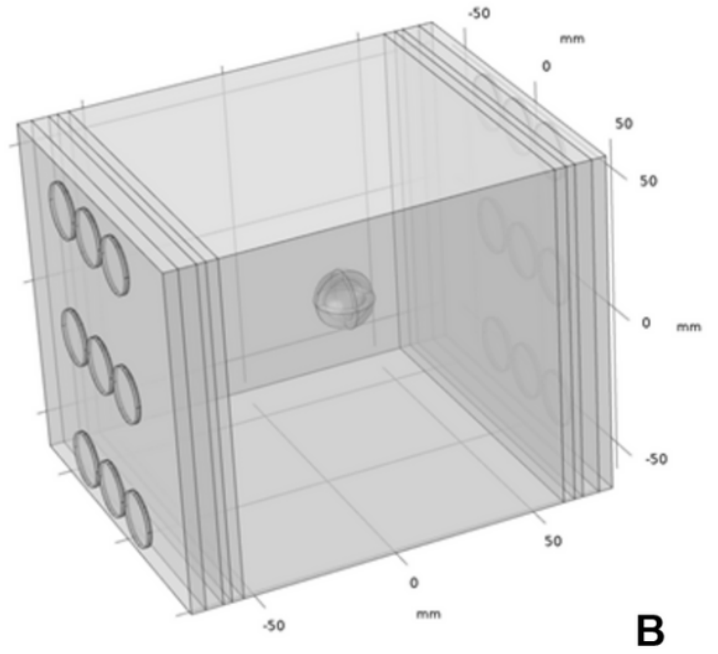
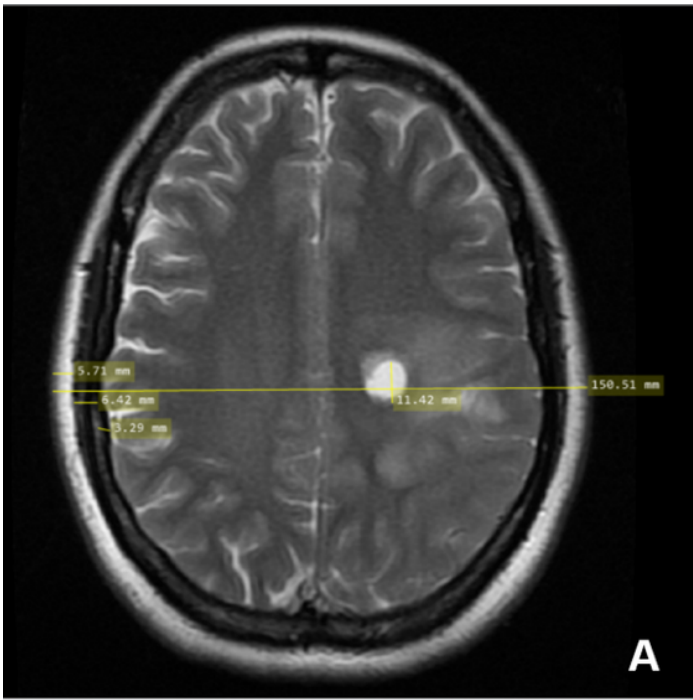


Figure 1

The scheme of constructing the MTL model. A. The patient's MRI data was measured for the design of MTL model. B. MTL model was constructed based on the patient's imaging data, and tumor was planted parallel to the center of TTFields array

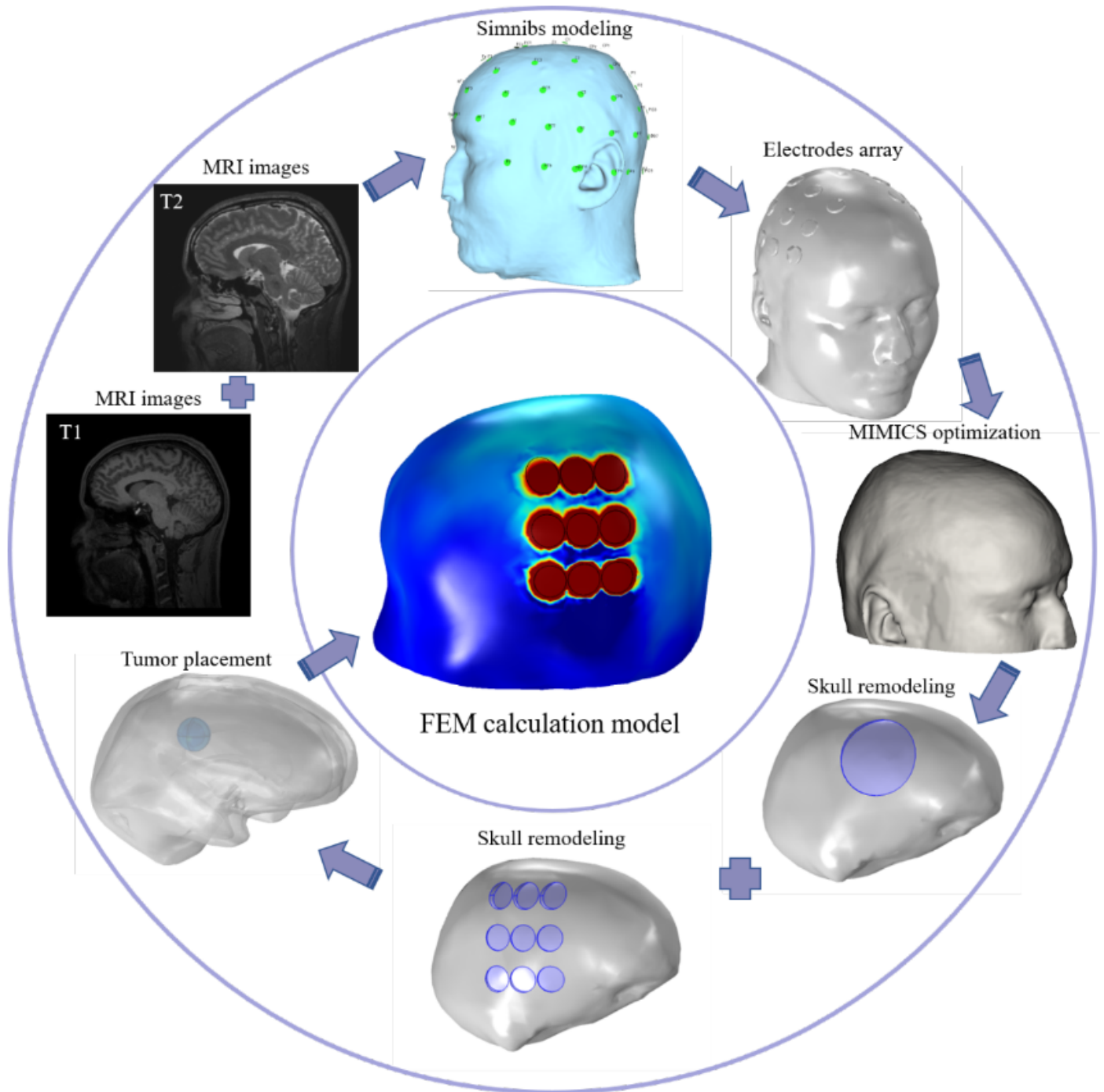


Figure 2

The establishment of head and brain tumor model by the finite element methods. MRI data was collected and extracted. Head model was constructed by SimNIBS and TFields array was placed at the specific sites. Then the head model was further optimized and smoothed. Skull remodeling was simulated in different configurations accordingly, and tumor was implanted parallel to the center of TFields array. Abbreviation: FEM, finite element methods; MRI, magnetic resonance imaging.

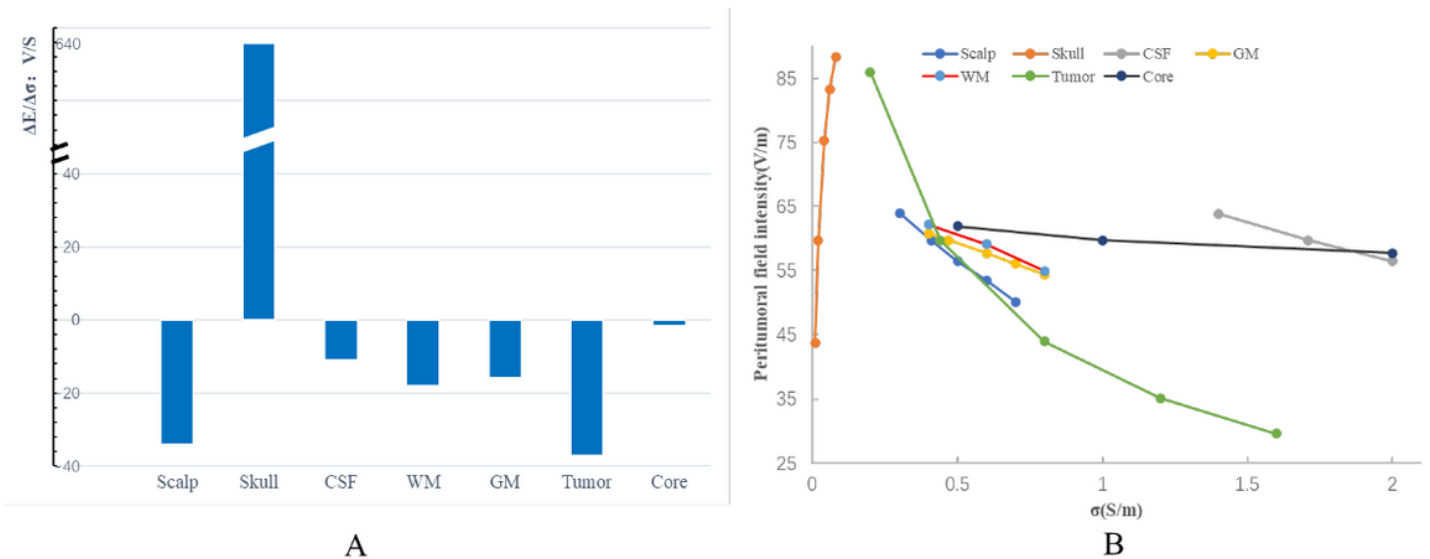


Figure 3

The conductivity of each layer of the head influenced the peritumoral field intensity. A. Histogram of peritumoral electric fields intensity variations along with each tissue's conductivity variations. B. Sensitivity analysis of peritumoral electric fields intensity along with each tissue's conductivity variations

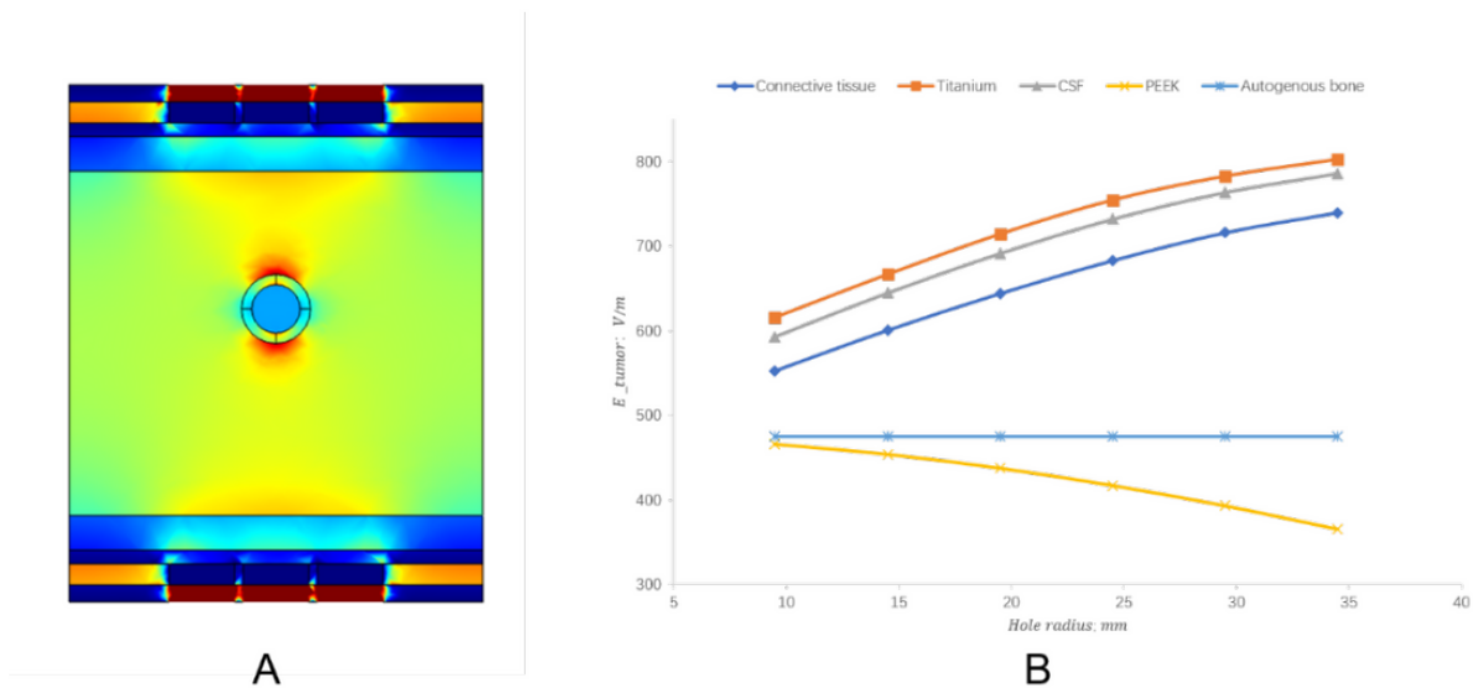


Figure 4

The size of single burr hole replaced by different material influenced the peritumoral field intensity. A. The simulated MTL model, where the different color pattern represents the distribution of the electrical intensity (red means higher intensity and blue means lower intensity). B. The change in API as altering the planted material and the size of the burr hole, where the titanium was superior in TTFields enhancement.

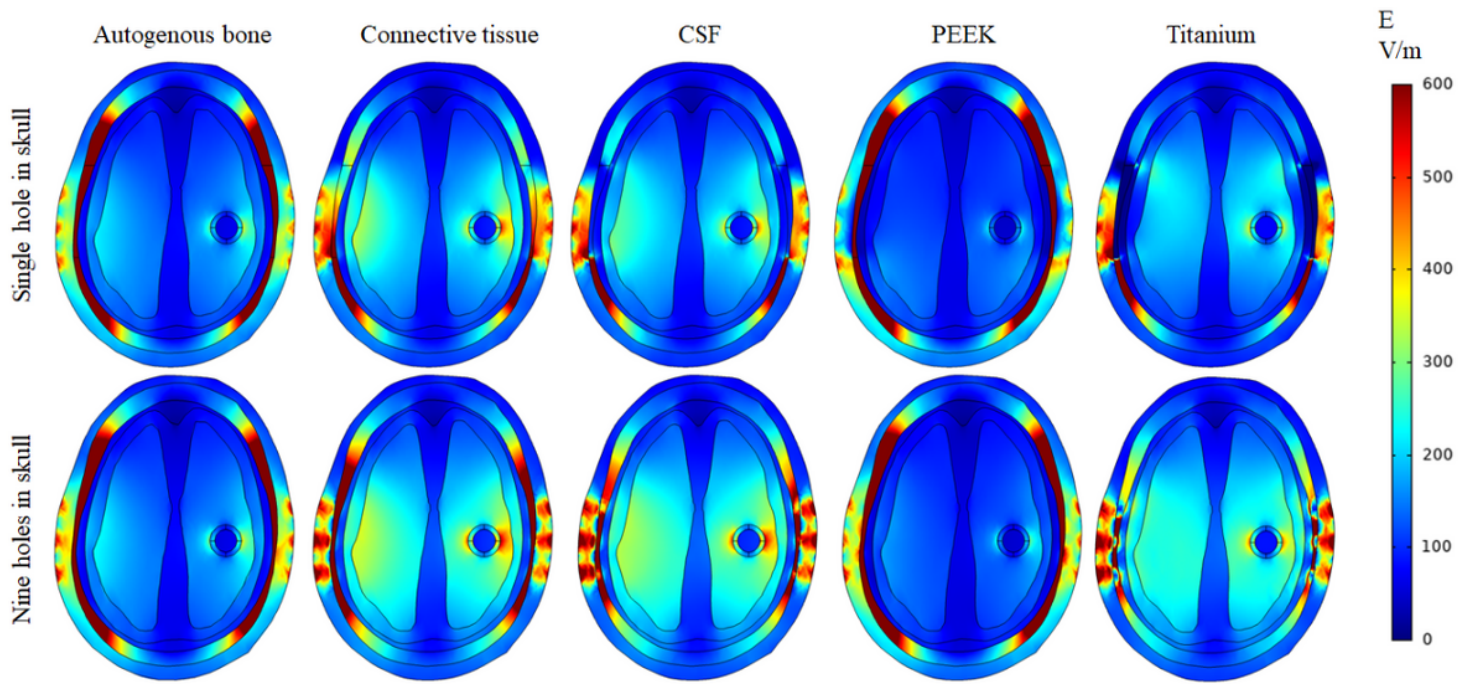


Figure 5

The implantation of bio-compatible materials and the pattern of the burr holes influenced the peritumoral field intensity. The skull drilling of a single hole compared to nine holes, and cranioplasty with different planted material were simulated in the RH model. In both drilling patterns, the connective tissue ranked the highest in TTFields enhancement, followed by CSF, the titanium, autologous bone, and PEEK. And nine burr holes in an array offered more enhancement to API, compared to a single burr hole in all models.

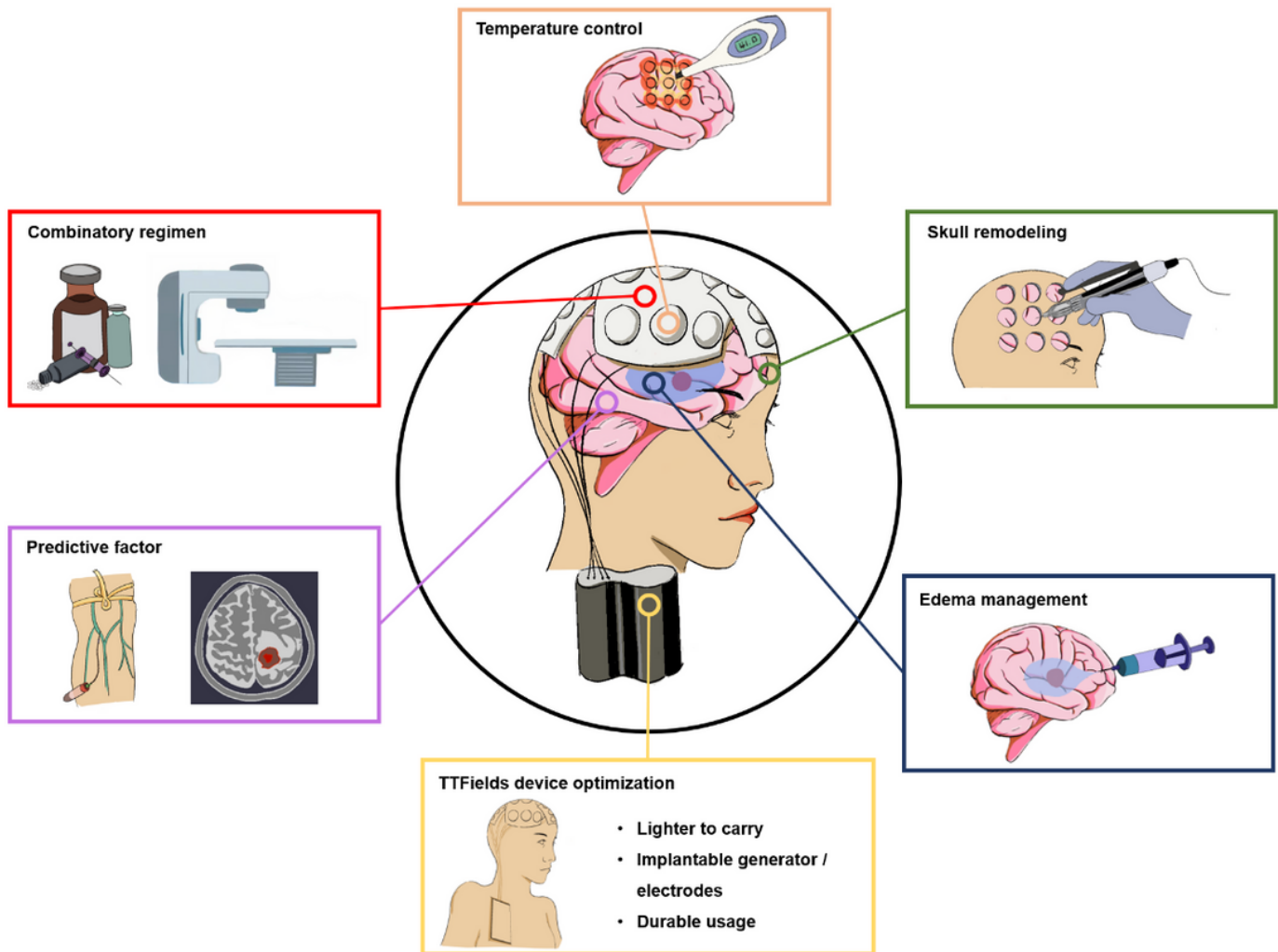


Figure 6

Potential perspective of TTFIELDS optimization The design of current TTFIELDS that are applied in the clinic warrants further optimization, including better temperature control of the electrodes, performing SR surgery to enhance TTFIELDS, and managing peritumoral edema to minimize its blocking effects. The devices also warrant further optimizing so that they can be lighter to carry, have implantable generators and electrodes, and be more durable in usage. Predictive factors from serum biomarkers and imaging markers are also required, and more combinatory regimens to augment TTFIELDS should be further explored.

Supplementary Files

This is a list of supplementary files associated with this preprint. Click to download.

- [Supplementarytables.docx](#)
- [Supplementaryfigures.docx](#)